Aerospace Science and Technology 45 (2015) 265–271

Contents lists available at ScienceDirect

Aerospace Science and Technology

www.elsevier.com/locate/aescte

A new GPS-based calibration of GRACE accelerometers using the arc-to-chord threshold uncovered sinusoidal disturbing signal

Andrés Calabia [a,b], Shuanggen Jin [a,c,*], Robert Tenzer [d]

[a] Shanghai Astronomical Observatory, Chinese Academy of Sciences, Shanghai 200030, China
[b] University of Chinese Academy of Sciences, Beijing 10047, China
[c] Department of Geomatics Engineering, Bulent Ecevit University, Zonguldak 67100, Turkey
[d] School of Geodesy and Geomatics, Wuhan University, Wuhan 430079, China

ARTICLE INFO

Article history:
Received 17 November 2014
Received in revised form 16 March 2015
Accepted 21 May 2015
Available online 27 May 2015

Keywords:
Accelerometers
Calibration
Global Positioning System (GPS)
Low Earth Orbit (LEO) satellites
Error analysis

ABSTRACT

In order to guarantee an unbiased solution in accelerometer measurements, calibration parameters have been finally calculated without using any kind of regularization or constraint. In this paper, a better calibration of the GRACE accelerometers is achieved from the instantaneous GPS-based non-gravitational accelerations. The first derivatives of the precise-orbit velocity are computed under an a priori arc-to-chord threshold, while the modelled time-varying forces of gravitational origin and reference-system rotations are computed according to current conventions (including sub-daily tide variations). After subtracting the modelled time-varying gravity from the GPS-based accelerations, cross-track axes of both GRACE satellites seem to be affected by a periodic error of unknown source. With the purpose of extracting the underlying information from the resulting data, the systematic error is modelled and subtracted successfully. According to this approach, the resulting accelerations serve as a reliable reference for accelerometer calibration.

1. Introduction

Considerable progress has been achieved over the last decade in improving the quality of available atmospheric and gravity models (e.g. [1–3]). Since their physical parameters can be derived from satellite accelerometer measurements (e.g. onboard GRACE), the non-gravitational accelerations are a promising source of information. An important topic of non-gravitational measurements is related to accelerometer calibration, and several methodologies have been developed and applied to compare computed non-gravitational accelerations with accelerometer measurements. For instance, the non-gravitational force models augmented with estimated empirical accelerations have shown a good agreement with accelerometer measurements [4]. Later, the non-gravitational force models were replaced with the accelerometer measurements in the reduced-dynamic POD, using a method which unfortunately needed strong constraints to be implemented in the cross-track and radial directions [5]. In [6], the non-gravitational accelerations were calculated as piece-wise constant empirical accelerations via the reduced-dynamic POD approach with a standard Bayesian weighted least-squares estimator. The regularization was applied to stabilize an ill-posed solution and only the longer wavelengths were recovered, at best in the along-track direction, with a bias in the cross-track direction. The authors concluded that no meaningful solution could be obtained in the radial direction.

Since accelerations can be derived from a numerical differentiation along precise orbits, the acceleration approach for accelerometer calibration aims on comparing the standard accelerations with the accelerometer readouts added to the time-varying gravity model. This approach is widely applicable because accelerations can be obtained from several accurate sources (e.g. kinematic GPS, SLR or Doppler solutions). Many discussions have been made about the choice of numerical derivative schemes to obtain standard accelerations, but none studied the repercussion of varying the data sampling interval in the simple three-point formula (1), e.g. [7–9]. For instance, the author of [9] tested different combinations of numerical second derivatives but concluded without arguments about the biases obtained. Nevertheless, the author demonstrated a successful method to de-correlate the residuals in accelerometer calibration using the generalized least squares method.

However, results of the above mentioned studies were limited not only by problems in the numerical differentiation, but also by the consequences of setting strong constraints or regularizations to solve correlated least-squares estimations. In this paper, a novel

* Corresponding author. Tel.: +86 21 34775292; fax: +86 21 64384618.
E-mail addresses: andres@calabia.com (A. Calabia), sgjin@shao.ac.cn (S. Jin).

http://dx.doi.org/10.1016/j.ast.2015.05.013
1270-9638/

Nomenclature

t_i	Instant i of time	GA/GB	Satellite identifier (GRACE-A/GRACE-B)
Δt	Increment of time	EOP	Earth Orientation Parameters
$\overline{C}_{lm}$	Normalized Stokes' coefficient of degree l and order m for cosine	MJD	Modified Julian Date
		UTC	Coordinated Universal Time
$\overline{S}_{lm}$	Normalized Stokes' coefficient of degree l and order m for sine	*TAI*	International Atomic Time
		ICRS	International Celestial Reference System
$\boldsymbol{\omega}_{\oplus}$	Rotation vector of the Earth	ITRS	International Terrestrial Reference System
$\boldsymbol{r}$	Satellite position vector	SBS	Satellite Body System
$\dot{\boldsymbol{r}}$	Satellite velocity vector	ORS	Orbit Reference System
$\ddot{\boldsymbol{r}}$	Satellite acceleration vector	$[P]$	Rotation matrix for precession
GPS	Global Positioning System	$[N]$	Rotation matrix for nutation
POD	Precise Orbit Determination	$[S]$	Rotation matrix for sidereal time
GRACE	Gravity Recovery And Climate Experiment	$[PM]$	Rotation matrix for polar motion

approach is developed and applied to accurately determine the instantaneous non-gravitational GPS-based accelerations. Since POD accelerations are not part of the available products at the Information System and Data Center (ISDC) *GeoForschungsZentrum* (GFZ) website, precise velocities have been interpolated and numerically differentiated. In order to derive the accurate total accelerations (gravitational + non-gravitational), orbital velocities have been interpolated under a priori arc-to-chord threshold defined by comparing accelerations calculated from different sampling interval. Finally, the instantaneous non-gravitational accelerations have been obtained by removing the time-varying gravity model. The advantage of using instantaneous non-gravitational accelerations instead arcs of orbits is the capability to analyze the differences to accurate accelerometer measurements. Within this context, our analysis has extracted a purely sinusoidal disturbing signal included in the POD solution to clarify the source for the correlations found by previous authors (e.g. [5] and [6]). Along with the benefit of using high accuracy and precise methodology and models, the systematic error has been modelled and removed from the computed non-gravitational accelerations, and the differences to accelerometer measurements directly estimated for accurate calibration. Additionally, the recovered amplitudes, phases and frequencies from the purely sinusoidal disturbing signal can be used in the future to study possible POD constrains.

2. Accelerometers and measurements

The GRACE is a joint partnership between the *National Aeronautics and Space Administration* (NASA) in the United States and the *Deutsches Zentrum für Luft und Raumfahrt* (DLR) in Germany, which has been widely used in geodesy and climate change applications (e.g. [10,2]). System development, data processing and archiving are shared between the *Jet Propulsion Laboratory* (JPL), *The University of Texas, Center for Space Research* (UTCSR) and the *GeoForschungsZentrum* (GFZ) in Potsdam.

In this study, 10 years' time-series (2002 to 2013) of Level 1B Format Record files have been downloaded from the ISDC website, after user registration and file request, using the Product Request List (PRL) format. Once the request was done, each file was downloaded from the ISDC ftp and processed automatically under MATLAB environment. Downloaded data files were read in big endian byte-ordering format [11], taking in account internal byte swaps and several bugs found, such as emptiness of file or wrong given values, among others.

2.1. Non-gravitational accelerometers (ACC_1B files)

Non-gravitational accelerations are obtained by measuring the force needed to keep a proof mass exactly at the spacecraft's centre of mass, where the gravity is exactly compensated by the centrifugal force. Plus and minus drive voltages are applied to electrodes with respect to opposite sides of the proof mass, whose electrical potential is maintained at a *dc* biasing voltage. Unfortunately, this *dc* level is the source of bias and bias fluctuations of the most electrostatic space accelerometers which are currently in use. The twin satellites of the GRACE mission are equipped with three-axis capacitive SuperSTAR accelerometers and their measurements, at a second interval, are included in the ACC_1B files.

2.2. Star Camera Assembly (SCA_1B files)

The star camera mounted on each satellite provides the precise attitude references to determine satellite's absolute orientation with respect to the ICRS. These measurements are given at a 5 s time-sampling interval, as a set of quaternion in the SCA_1B files.

2.3. POD of GRACE (GNV_1B files)

Within the process of deriving satellite accelerations from GPS observations, the reduced-dynamic Precise Orbit Determination (POD) approach is the most complete and accurate strategy. Computed by the GPS Inferred Positioning System (GIPSY) software of JPL, the GNV_1B files provide the most precise position and velocity at 5 s interval, including formal error.

3. Methods and processing

In order to implement an acceleration approach, the satellite's total acceleration is derived from the precise orbits by means of interpolation and subsequent numerical differentiation. Then, accelerations of gravitational origin are computed and subtracted in the same reference system. Finally, the analysis, modelling and subtraction of accidental and systematic errors are conducted.

3.1. Satellite's total acceleration

Total accelerations are obtained numerically as the first derivative of the GNV_1B velocities. When calculating total accelerations by a simple differentiation of velocities, the first approximations to numerical derivatives have been found to produce large bias [9]. This bias is caused by the arc-to-chord approximation derived from (1). To avoid this error of approximation, the interpolated GNV_1B velocities must be differentiated by an increment of time (Δt) which minimizes the error committed at a given threshold. The three-point formula, here also written in the form of the two-velocity formula, is given by

Table 1
Arc-to-chord approximation error in GRACE orbit.

Δt (s)	Error (nm/s^2)
0.05	1
0.1	3
0.2	12
0.5	50
1	120
2	1500

$$\ddot{\boldsymbol{r}}_{t_0} = \lim_{\Delta t \to 0} \ddot{\boldsymbol{r}}''_{t_0} = \lim_{\Delta t \to 0} \frac{\dot{\boldsymbol{r}}'_{t_1} - \dot{\boldsymbol{r}}'_{t_{-1}}}{\Delta t} = \lim_{\Delta t \to 0} \frac{\boldsymbol{r}_{t_2} - 2\boldsymbol{r}_{t_0} + \boldsymbol{r}_{t_{-2}}}{(\Delta t)^2} \quad (1)$$

where simple and double quotation mark denotes simple or double of arc to chord approximation respectively, and each t_i is equispaced by Δt. Eq. (1) itself is the definition of the instantaneous acceleration. In a non-linear trajectory, the instantaneous velocity can't be calculated as a simple difference between two positions without taking into account the error associated to the non-linear path. Between two instantaneous velocities, the instantaneous acceleration neither. Following this, a precise numerical approximation can be achieved by minimizing the increment of time up to a desired accuracy. Then, the threshold of accuracy can be implemented by comparing the accelerations obtained in each test of increments. Centripetal accelerations from angular velocities and radius of three-point-fitted circles were also tested and provided unbiased results, but with several large discrepancies probably caused by the nature of the non-circular orbit configuration.

In order to keep the error of interpolation small enough, a low-degree polynomial is not sufficient, high-degree polynomials introduce undesired oscillations, and the FFT approach is not considered in presence of data gaps and outliers [12]. The best alternative, as demonstrated in [7], is to use a piece-wise interpolation, such as splines or Hermite polynomials. In this study, different algorithms were compared, interpolating odd from even original samples, and the committed error evaluated by a simple difference between interpolated and original data. Finally, 8-data point piece-wise Lagrange interpolation was chosen, which provided a white noise error of standard deviation of ∼10 nm/s, from evaluating the error committed at 10 s sampling (odd from even original samples). Similar results were obtained when testing the piecewise cubic Hermite interpolation. Since the derivatives given as an output in our tested algorithms did not provide enough accuracy, the two-velocity formula (1) was used under an a priori arc-to-chord threshold to obtain more accurate and unbiased accelerations. In this way, total accelerations were calculated for several Δt and a value of 0.05 s was chosen for Δt, giving an error smaller than 1 nm/s^2 in the arc-to-chord approximation. In other words, by comparing the accelerations calculated from different sampling interval, the arc-to-chord threshold was fixed to 0.05 s. Using a bigger sampling interval in the two-velocity formula (1), the biases obtained in each test were bigger than the required accuracy (∼1 nm/s^2). GRACE values for the biases accumulated with respect to the threshold are shown in Table 1.

3.2. Gravitational accelerations

The conventional gravity model based on the EGM2008 [13], describes with Stokes' coefficients the static part of the gravitational field and the underlying background for the secular variations of its $\bar{C}_{20}$, $\bar{C}_{21}$, $\bar{S}_{21}$, $\bar{C}_{30}$ and $\bar{C}_{40}$ coefficients. In addition, when computing the gravitational forces acting on the user's satellite, other time-varying effects must be also taken into account. These include the third body tide caused by the Moon and Sun [14], the solid Earth tides [13], the ocean tides [15], the solid Earth pole tide [13], the ocean pole tide [16] and the relativistic terms [13].

Time-varying Stokes' coefficients up to a degree and order of 120 were computed (including sub-daily variations) under an increment of time small enough to desensitize from discontinuities (∼3600 s). Then, the gravity was calculated, for every satellite position, using the first derivative of the gravitational potential in Cartesian coordinates [17].

3.3. Reference systems

In order to compute the differences between the GPS-based non-gravitational accelerations and the accelerometer measurements, several transformations between reference systems are required (POD solutions are usually given in the ITRS and accelerometer measurements in the SBS). The rotation from ICRS to SBS [17] was derived from the star-camera quaternion, while the rotation from ITRS to ICRS [13] was realized according to the well-known expressions

$$\boldsymbol{r}_{ICRS} = [P][N][S][PM]\boldsymbol{r}_{ITRS} \quad (2)$$

$$\dot{\boldsymbol{r}}_{ICRS} = [P][N][S]\left\{[PM]\dot{\boldsymbol{r}}_{ITRS} + \boldsymbol{\omega}_{\oplus} \times [PM]\boldsymbol{r}_{ITRS}\right\} \quad (3)$$

Time conversion between the given time in Level 1B files and the *UTC* can be found in the GRACE Level 1B Data Product User Handbook [11]. Therefore, EOP were computed at the GNV_1B sampling for further processing. Since the sub-daily polar motion (p_x, p_y), Universal Time (*UT1*) and Length of Day (*LOD*) variations [13] are not a part of the EOP 08 C04 values reported at the IERS website [18], they were added only after interpolation. Diurnal and semi-diurnal ocean tides and nutation contributions were computed and added to the interpolated EOP [13].

Furthermore, the GNV_1B positions and velocities were rotated to the ICRS [(2) and (3)] by using the computed sub-daily EOP. Then, the GPS-based accelerations were computed on the ICRS as previously has been detailed and the direct tides calculated from the Sun and Moon ICRS coordinates. Sun and Moon coordinates were also rotated to the ITRS (2) to compute the frequency-independent solid tides [13]. Then, gravitational accelerations were rotated to the ICRS by using (2) (as they were positions) and the differences to GPS-based accelerations were rotated to the SBS.

3.4. Modelling a systematic error in Y_{SBS} axes

The advantage of using instantaneous non-gravitational accelerations instead arc of orbits is the capability to analyze the differences to accurate accelerometer measurements. For instance, in Fig. 3 the X_{SBS} axes in grey line shows a white noise of ∼10 nm/s^2 with respect to the accelerometer measurements (black, cyan and magenta lines are the same measurements but biased by different author's parameters). Concerning the Y_{SBS} axes, an unknown periodic error of amplitude maxima of ∼3 μm/s^2 was identified for both GRACE satellites (e.g. Fig. 1). Z_{SBS} axes also revealed a slightly systematic behaviour, but two orders of magnitude smaller (e.g. Fig. 1). After a strong review seeking for the provenance of this error and seeing that only the Y_{SBS} axis of both satellites were affected, it was decided to remove it, especially when the same pattern was seen in other author's figures [9, Fig. 7].

A periodic behaviour of its varying amplitude suggested the fitting by sinusoidal functions based on applying a robust least-squares regression analysis. The robust linear fitting M-estimator method Tukey's biweight (also known as bisquare) was applied to avoid outlines. The main idea was to recover the underlying signal by subtracting a sinusoidal function fitted on the envelope of the modulated amplitude. A first function would regularize the envelope of the modulated amplitude of which shape was approximated by an elaborated smoothing computed over the 5 s

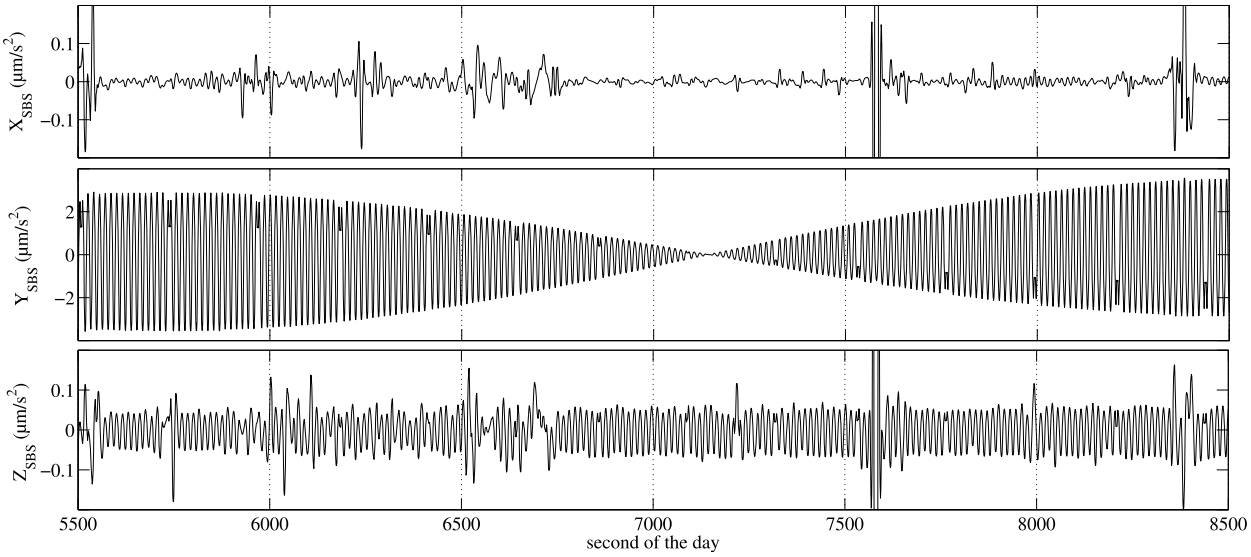

Fig. 1. Residuals from removing the systematic error on axis Y_{SBS} and smoothing the solution. The periodic behaviour of varying amplitude of Y_{SBS} can also be seen in [9, Fig. 7]. Results for both satellites are similar. Plots are not equally scaled.

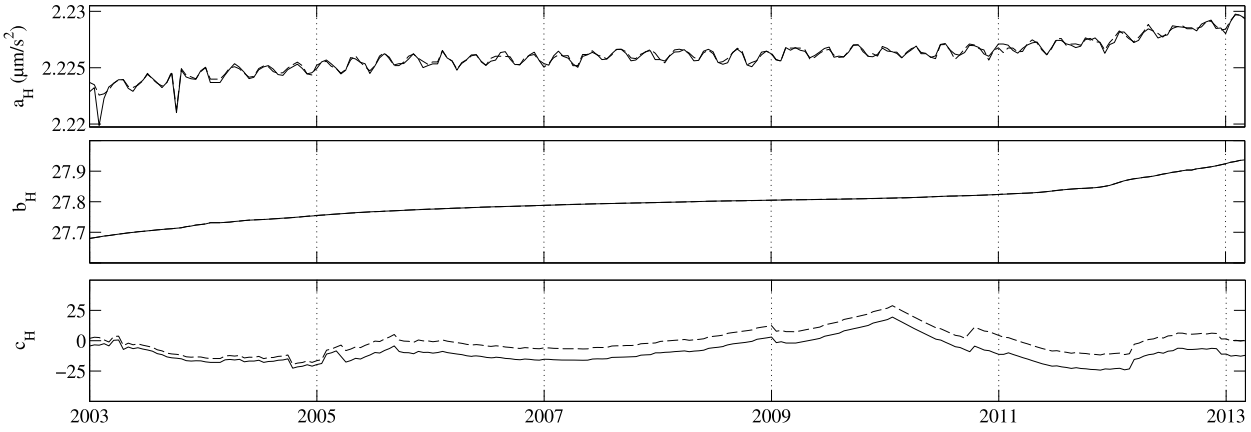

Fig. 2. Fitted parameters – dashed line for GA and solid line for GB – of the sinusoidal function f_H, which removes the systematic error on Y_{SBS} axes. Parameters of function f_L are not plotted because they are similar but with amplitude of ∼0.65 μm/s^2. Here, $f_i = \mathrm{a} \cdot \sin(\mathrm{b}x + \mathrm{c})$, for $i = H, L$ and $x = (x' - mean(x'))/std(x')$ is the normalization by mean and standard deviation of $x' = \mathrm{JD}(UTC) - 2.455E6$.

sampling solution. The second function, an envelope of modulated amplitude, was approximated by subtracting the smoothed GPS-based non-gravitational accelerations from non-smoothed ones. The modulating envelope was approximated from absolute values multiplied by a ±1 binary function, computed from positive or negative values of the first function.

Two daily functions $f_i = \mathrm{a} \cdot \sin(\mathrm{b}x + \mathrm{c})$, for $i = H, L$, were fitted to the approximated results. Fig. 2 shows the temporal behaviour of the fitted parameters. To apply the corrections, the first function (f_L) was directly subtracted from the GPS-based non-gravitational accelerations and converted into binary (±1) function for the next step. Absolute values of the resulting data were then multiplied by this binary function, while the second function (f_H) was removed. Results for two different days are shown in Fig. 3. Since only sinusoidal functions have been removed, the resulting solution remains unchanged from mean values and, consequently, the Y_{SBS} bias estimation.

4. Results and discussion

In this paper, the acceleration approach for accelerometer calibration has been conducted by comparing numerically differentiated orbital velocities with the accelerometer readouts added to the time-varying gravity model. Instantaneous non-gravitational accelerations were calculated for the 10-year time series (2003 to 2013) and their biases to accelerometer outputs simply differenced from their daily-median-averaged values (scale seems not to be affected). In Table 2, the fitted biases by polynomial functions are summarized for four separate data spans.

Calibration parameters from [19] and [9] were also included and all plotted in Fig. 4 with respect to the a priori parameters as recommended by [20]. For these authors, pre-processing was needed to synchronize dates, remove outlines and interpolate data gaps. In Fig. 4, it can be seen a good agreement with the X_{SBS} bias from [19], these solutions are smoother than [9]. On the other hand, Y_{SBS} and Z_{SBS} biases better follow solutions of [9]. Since the nature of circular orbits implies a constant behaviour of the arc-to-chord error, the real magnitude (bigger) of radial accelerations (Z_{SBS} axes) seems to cause a constant difference (∼20 nm) to the solutions of [9] and [20]. In general terms, the results show that [19] and [20] are worse in calibrating Y_{SBS} and X_{SBS} respectively. The difference with respect to the solutions of [19] for Z_{SBS} axes is still under analysis. In Fig. 4, it is interesting to see that since electrostatic accelerometers are sensible to temperature changes, the correlation between Y_{SBS} biases and the β' angle (angle between the Earth–Sun line and the orbit plane) is clearly recognized. Note

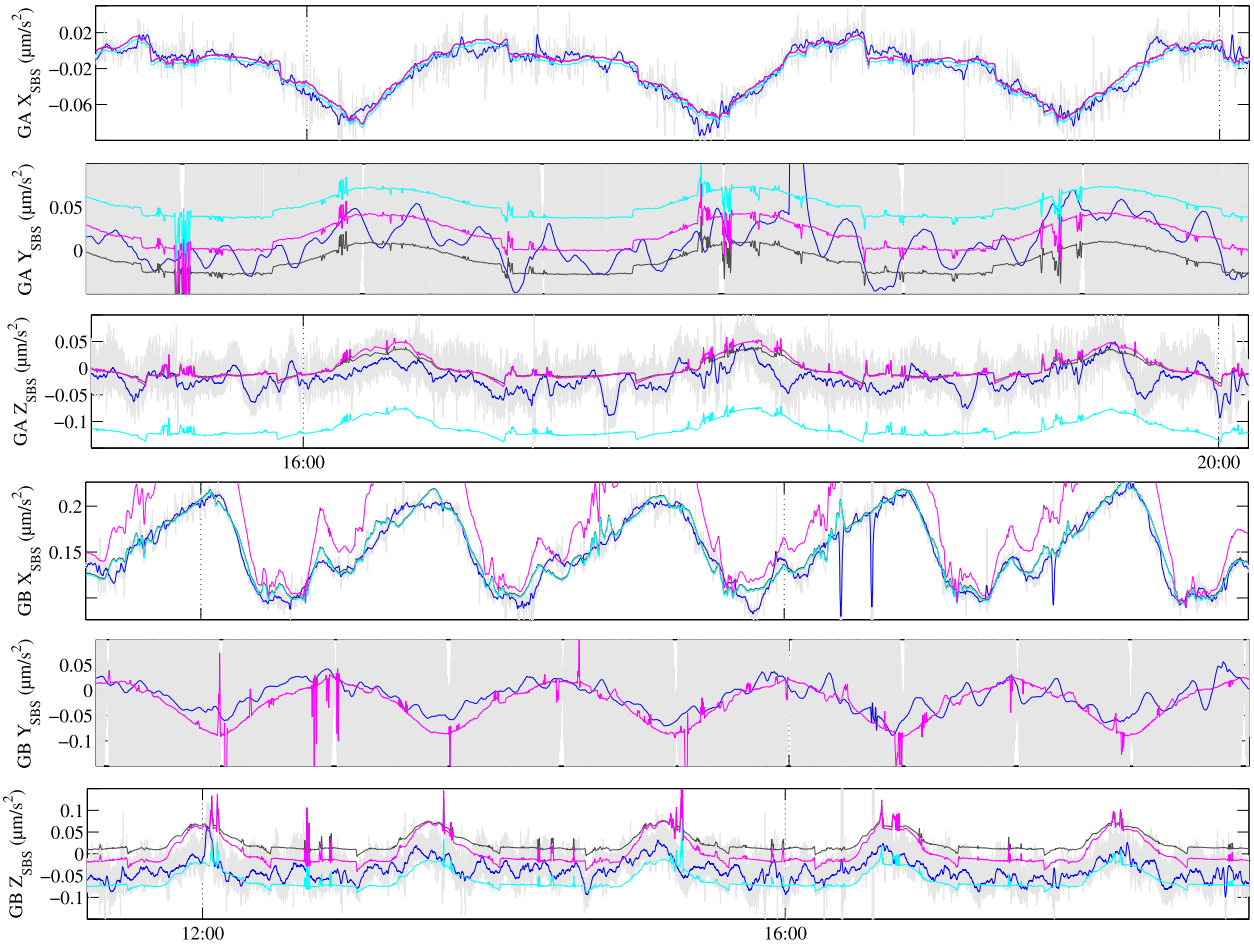

Fig. 3. Measured non-gravitational accelerations calibrated by [20] in black, by [19] in cyan and by [9] in magenta and the GPS-based non-gravitational accelerations from this study in blue. Gray line shows the data of previous systematic error removal (in Y_{SBS} axes it is obviously too big) and smoothing. GA on July 15th, 2006 is shown in the upper part and GB on January 15th, 2003 in the lower part. Plots are not equally scaled. (For interpretation of the references to colour in this figure legend, the reader is referred to the web version of this article.)

Table 2
Fitted parameters for bias calibration of GRACE accelerometers.

Axis		Time span in MJD(*UTC*)			
		52 720–53 720	53 720–55 390	55 390–55 670	55 670–56 276
X_{SBS} GA	a	1.8661E−10	7.6744E−11	2.6610E−09	−2.1745E−09
	b	3.7589E−09	−1.2267E−09	3.4110E−09	2.0266E−08
	c	−1.2067E−06	−1.2572E−06	−1.2949E−06	−1.3772E−06
X_{SBS} GB	a	1.3180E−10	−3.6244E−12	−3.1007E−10	7.3652E−10
	b	3.1492E−09	−1.5015E−09	−1.0071E−09	−7.1242E−09
	c	−5.9029E−07	−6.3587E−07	−6.5277E−07	−6.6374E−07
Y_{SBS} GA	a	−7.3899E−09	−8.6972E−10	−3.6298E−08	2.1178E−08
	b	−2.3187E−07	4.1156E−09	−6.5976E−08	−2.1715E−07
	c	2.7577E−05	2.9751E−05	3.0619E−05	3.2154E−05
Y_{SBS} GB	a	−1.2166E−08	−1.9175E−09	2.4402E−08	2.7737E−08
	b	−3.9671E−07	2.0905E−08	4.5169E−08	−2.3808E−07
	c	7.4314E−06	1.1700E−05	1.2362E−05	1.3520E−05
Axis		Time span in MJD(*UTC*)			
		52 720–53 005	53 005–55 166	55 166–55 562	55 562–56 276
Z_{SBS} GA	a	2.5641E−09	4.1747E−11	6.9776E−10	−7.2715E−12
	b	1.3726E−07	7.7995E−10	1.1175E−09	−1.3730E−09
	c	1.2378E−06	−5.6749E−07	−5.7292E−07	−6.0213E−07
Axis		Time span in MJD(*UTC*)			
		52 720–53 005	53 005–55 287	55 287–55 562	55 562–56 276
Z_{SBS} GB	a	3.9394E−09	−5.8487E−11	−1.9218E−09	7.5564E−10
	b	2.1614E−07	3.0758E−09	1.3300E−09	−4.9383E−09
	c	2.0507E−06	−7.3738E−07	−7.5710E−07	−7.7023E−07

Equation: $bias = ax^2 + bx + c$, where $x = (\mathrm{MJD}(UTC) - 55\,555)/100$.

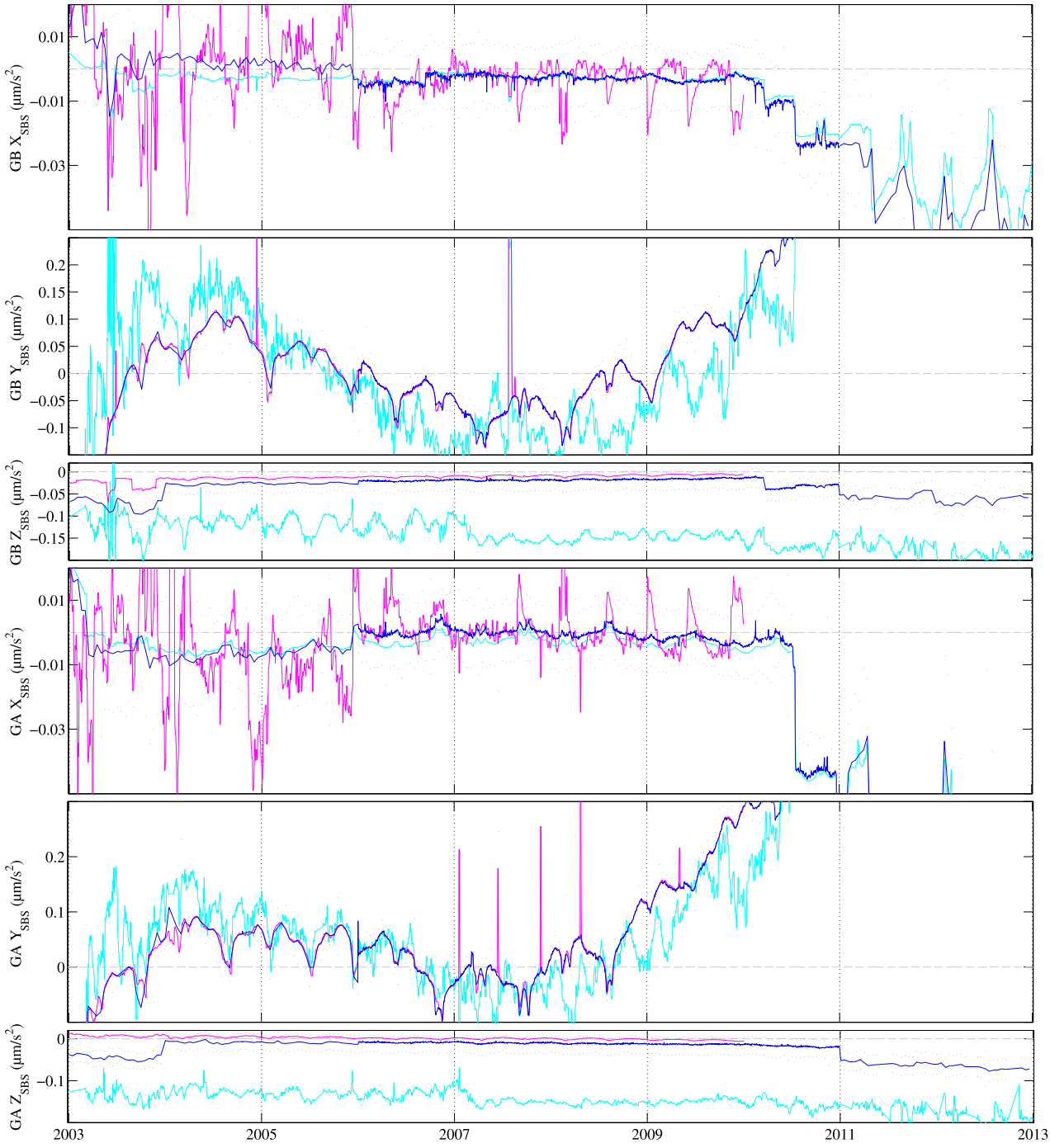

Fig. 4. Differences with respect to [20]: results from [19] are shown in cyan, from [9] in magenta and this study in blue. Dotted blue line shows the standard deviation for the daily residuals of the GPS-based non-gravitational accelerations after calibration has been done to accelerometer measurements. Plots are not equally scaled. (For interpretation of the references to colour in this figure legend, the reader is referred to the web version of this article.)

here that the β' angle is defined such that it is zero when the Sun is within the orbit plane and, consequently, the perturbation of Y_{SBS} biases is minimized. The opposite situation happens maximum β' angle, in which the solar radiation has the same direction as the Y_{SBS} axes and maximizes its bias perturbation. These variations are disregarded in the polynomial fitting given in Table 2, being this solution a more close approximation to values of β' angle zero than the real β' angle value. The evolution of β' angle values can be seen at the website of the *University of Texas, Center for Space Research* (UTCSR).

When analyzing the solution for X_{SBS} axes, aside the excellent agreement with the precision of the accelerometer, several local discrepancies can be identified. These differences can probably be attributed to the omitted atmospheric tides, non-modelled local time-varying gravity (such as post glacial rebound, hydrologic cycle, etc.), lack of accuracy of ocean tides models or possible external sources to the Earth's gravity, e.g. Fig. 3 (upper panel) at 19:30 h.

Biases can be differenced in four separate data spans, as shown in Table 2. For X_{SBS} and Y_{SBS} axes of both GRACE satellites, the changes of bias are clearly defined when satellite positions were swapped in December 2005 and from possible manoeuvres at the end of mission, in July 2010 and April 2011. As seen, both satellite Z_{SBS} axes were not affected from swapping positions but, instead,

there is a change at common dates in January of 2004 and 2011. During a middle–end mission, Z_{SBS} biases changed in December 2009 for GA and April 2010 for GB. All these approximate dates are seen in the MJD format in Table 2.

Concerning the results from the systematic error found on the Y_{SBS} axes, note that there is a high correlation between its frequency, amplitude and phase (e.g. Fig. 2) and the magnitude of the orbital semi-major axis, inclination and inflexion points of eccentricity satellite orbit respectively. Note that the evolution of GRACE mean orbits can be found at the UTCSR website.

5. Conclusions

With the development of space accelerometers, the calibration of current bias-rejection devices is not anymore required. Nevertheless, it has been demonstrated that the non-gravitational accelerations can be determined accurately from the precise orbit ephemeris and, so far, it is, among others, a precious source of information for atmospheric studies. In order to guarantee an unbiased solution in accelerometer measurements, calibration parameters have been calculated without using any kind of regularization or constraint, by using the GPS-based POD solution as a reference. Since POD accelerations are not usually given as a part of the POD products, here is given a feasible methodology with the use of the arc-to-chord threshold for data differentiation. This approach is widely applicable because accelerations can be obtained from several accurate sources (e.g. kinematic GPS, SLR or Doppler solutions). After subtracting the modelled time-varying gravity from the GPS-based accelerations, cross-track axes of both GRACE satellites are affected by a periodic error of unknown source. With the finality of extracting the underlying information, the disturbing signal has been modelled and subtracted successfully by applying the sinusoidal robust fitting. The results show excellent agreement with the accelerometer measurements and demonstrate that this new approach is a good reference for accelerometer calibration. Concerning the systematic error found, it is clear that a purely sinusoidal disturbing signal should have been already removed from the ISDC products and it should have further considerations in future POD software development.

Since recent advances in the-state-of-the-art of time-varying gravity field models and GPS-derived accelerations seem to provide wide expectations on many branches of research, future investigations could address, but are not restricted to, the studies of (i) tests with kinematic data, (ii) differences to GIPSY–OASIS accelerations, (iii) POD constrains for the purely sinusoidal disturbing signal or (iv) validation of the time-varying gravity model with accelerometer measurements, among others.

Conflict of interest statement

The authors declare that there is no conflict of interest regarding the publication of this paper.

Acknowledgements

This work was supported by the National Keystone Basic Research Program (MOST 973) (Grant No. 2012CB72000), Main Direction Project of Chinese Academy of Sciences (Grant No. KJCX2-EW-T03), Shanghai Science and Technology Commission Project (Grant No. 12DZ2273300), National Natural Science Foundation of China (NSFC) Project (Grant Nos. 11173050 and 11373059) and Key Laboratory of Planetary Sciences, Chinese Academy of Sciences. Great appreciation is extended to the ISDC for providing the data access and special thanks are given to Dr. Sean Bruinsma and Dr. Ales Bezdek for communication and discussion.

References

[1] S. Bruinsma, D. Tamagnan, R. Biancale, Atmospheric densities from CHAMP/STAR accelerometer observations, Planet. Space Sci. 52 (4) (March 2003) 297–312.
[2] S.G. Jin, T. van Dam, S. Wdowinski, Observing and understanding the Earth system variations from space geodesy, J. Geodyn. 72 (Dec. 2013) 1–10.
[3] S.G. Jin, E. Cardellach, F. Xie, GNSS Remote Sensing: Theory, Methods and Applications, Springer, Netherlands, 2014.
[4] T. Van Helleputte, P. Visser, GPS based orbit determination using accelerometer data, Aerosp. Sci. Technol. 12 (6) (Sept. 2008) 478–484.
[5] T. Van Helleputte, E. Doornbos, P. Visser, CHAMP and GRACE accelerometer calibration by GPS-based orbit determination, Adv. Space Res. 43 (12) (June 2009) 1890–1896.
[6] J. Van den Ijssel, P. Visser, Performance of GPS-based accelerometry: CHAMP and GRACE, Adv. Space Res. 39 (10) (2007) 1597–1603.
[7] T. Reubelt, M. Götzelmann, E.W. Grafarend, Harmonic analysis of the Earth's gravitational field from kinematic CHAMP orbits based on numerically derived satellite accelerations, in: Observation of the Earth System from Space, Part I, Springer-Verlag, Berlin, Heidelberg, 2006, pp. 27–42.
[8] P. Ditmar, V. Kuznetsov, A.A.V.E. van der Sluijs, E. Schrama, R. Klees, DEOS CHAMP-01C70′: a model of the Earth's gravity field computed from accelerations of the CHAMP satellite, J. Geod. 79 (10–11) (Dec. 2006) 586–601.
[9] A. Bezděk, Calibration of accelerometers aboard GRACE satellites by comparison with POD-based nongravitational accelerations, J. Geodyn. 50 (5) (Dec. 2010) 410–423.
[10] S.G. Jin, L.J. Zhang, B.D. Tapley, The understanding of length-of-day variations from satellite gravity and laser ranging measurements, Geophys. J. Int. 184 (2) (Oct. 2011) 651–660.
[11] GRACE Level 1B Data Product User Handbook, JPL Publication D-22027, 2002.
[12] M. Weigelt, N. Sneeuw, Numerical velocity determination and calibration methods for CHAMP using the energy balance approach, in: Int. Assoc. Geod. Symp., vol. 129, 2005, pp. 54–59.
[13] G. Petit, B. Luzum, IERS conventions (2010), IERS technical note 36, International Earth Rotation and Reference Systems Service (IERS), Verlag des Bundesamts für Kartographie und Geodäsie, Frankfurt am Main, 2010.
[14] O. Montenbruck, E. Gill, Satellite Orbits – Models, Methods and Applications, Springer-Verlag, Berlin, Heidelberg, New York, 2000.
[15] D. Rieser, et al., The ocean tide model EOT11a in spherical harmonics representation, available online at: ftp://ftp.dgfi.badw.de/pub/EOT11a, July 2012.
[16] S.D. Desai, Observing the pole tide with satellite altimetry, J. Geophys. Res. 107 (C11) (2002) 3186, data available online at: http://62.161.69.131/iers/conv2010/convupdt/convupdt_c6.html.
[17] B. Frommknecht, Integrated Sensor Analysis of the GRACE Mission, DGK, Reihe C, Heft 617, Verlag der Bayerischen Akademie der Wissenschaften, 2008.
[18] C. Bizouard, D. Gambis, The combined solution C04 for Earth orientation parameters consistent with International Terrestrial Reference Frame 2008, International Earth Rotation Service, available online at: http://hpiers.obspm.fr/iers/eop/eopc04/eopc04.62-now, Sept. 2014.
[19] S. Bruinsma, R. Biancale, F. Perosanz, Calibration parameters of the CHAMP and GRACE accelerometers, CNES Poster Commun., 2007.
[20] S. Bettadpur, Recommendation for a-priori bias & scale parameters for Level-1B ACC data, GRACE technical note No. 2, V.2, available online at: ftp://podaac.jpl.nasa.gov/allData/grace/docs/TN-02_ACC_CalInfo.pdf, June 2009.